Liquid-Liquid Separation of Aqueous Solutions: A Molecular Dynamics Study

Takuma Yagasaki,[a] Masakazu Matsumoto, and Hideki Tanaka[b]

Research Institute for Interdisciplinary Science, Okayama University, Okayama, 700-8530, Japan

[a] E-mail: t.yagasaki@gmail.com

[b] E-mail: htanakaa@okayama-u.ac.jp

In the liquid-liquid phase transition scenario, supercooled water separates into the high density liquid (HDL) and low density liquid (LDL) phases at temperatures lower than the second critical point. We investigate the effects of hydrophilic and hydrophobic solutes on the liquid-liquid phase transition using molecular dynamics simulations. It is found that a supercooled aqueous NaCl solution separates into solute-rich HDL and solute-poor LDL parts at low pressures. By contrast, a supercooled aqueous Ne solution separates into solute-rich LDL and solute-poor HDL parts at high pressures. Both the solutes increase the high temperature limit of the liquid-liquid separation. The degree of separation is quantified using the local density of solute particles to determine the liquid-liquid coexistence region in the pressure-temperature phase diagram. The effects of NaCl and Ne on the phase diagram of supercooled water are explained in terms of preferential solvation of ions in HDL and that of small hydrophobic particles in LDL, respectively.

INTRODUCTION

The liquid-liquid phase transition scenario explains various anomalous properties of water such as the sharp increase in specific heat with decreasing temperature and the apparently first order transition between two amorphous ices induced by pressure.[1–8] In this scenario, liquid water under ambient condition is considered as a supercritical fluid. There exists a coexistence line between the high density liquid (HDL) phase and the low density liquid (LDL) phase in the pressure-temperature plane, and this coexistence line is terminated at a critical point in the deeply supercooled region. There has been no direct experimental evidence for the liquid-liquid critical point of bulk water because liquid water crystallizes very quickly. However, experiments of amorphous ice and confined water support the liquid-liquid phase transition scenario.[9–16]

Molecular dynamics (MD) simulations are useful to investigate deeply supercooled water because it is possible to examine processes that are faster than homogeneous nucleation of ice (the induction time for nucleation of ice I is longer than the timescale of typical MD simulations unless monoatomic water models or biased simulation techniques such as the forward-flux sampling method are employed).[17–24] If liquid water separates into two liquid phases and the curvature of the interface dividing the two phases is low enough, the isotherm of pressure plotted against density becomes flat, i.e., $(\partial P/\partial \rho)_T = 0$ (a van der Waals loop would be observed for small cubic simulation cells in which the interface cannot be flat). The critical temperature is the highest temperature at which the plateau of the isotherm is observed. The location of the liquid-liquid critical point in the phase diagram have been determined by this method for various water models.[2,25–30] More sophisticated computational techniques such as free energy calculations and finite size scaling have also been used to investigate the liquid-liquid critical point of water.[31–37]

In a previous study, we performed MD simulations of the ST2, TIP5P, and TIP4P/2005 water models and observed spontaneous liquid-liquid separation at temperatures lower than the liquid-liquid critical point of the employed model.[38] The time scale of the separation is two orders of magnitude shorter than that of crystallization of ice for ST2 water. Guo *et al.* reported that the liquid-liquid separation of ST2 water occurs in large systems up to 256,000 molecules.[39]

Experimental studies have suggested that the liquid-liquid separation is not a unique property of pure water. Angell and Sare postulated that aqueous LiCl solutions separate into two immiscible liquid phases on the basis of DTA results.[40] A series of experiments by Suzuki and Mishima supports strongly the existence of the liquid-liquid separation of aqueous LiCl solutions.[41–44]

Recent experimental studies suggest that liquid-liquid transition occurs in a hydrazinium trifluoroacetate solution[45] and various aqueous alcohol solutions.[46–50] Most of the experimental studies measured properties of vitrified aqueous solutions at temperatures near or lower than the crystallization temperature, $T_x \sim 150$ K, at which amorphous ice crystallizes into ice I by heating. Therefore, the details of the phase behavior of aqueous solutions near the liquid-liquid critical point of pure water, $T_{c'} \sim 220$ K,[11,51–53] is still unclear.

There are several theoretical and computational studies of the phase behavior of supercooled aqueous solutions.[54–62] Paschek calculated the excess chemical potential of Ar in TIP5P-E water using the particle insertion method and found that the solubility of Ar in LDL is much higher than that in HDL.[62] Le and Molinero performed MD simulations of an aqueous solution of hydrophilic particles using a coarse-grained model.[58] The solute molecule was modeled so that it does not prefer tetrahedral coordination in water. They demonstrated that the solution separates into solute-rich and solute-poor parts and becomes nanosegregated glass at low temperatures for a range of solute concentration. Corradini *et al*. calculated the isotherms of pressure using MD simulations for several solution systems.[54–57] They showed that the liquid-liquid critical point shifts to lower pressures and higher temperatures as the concentration of NaCl increases.[54,55]

The liquid-liquid coexistence conditions of pure water is represented by a line in the pressure-temperature plane, whereas the coexistence conditions of an aqueous solution should be a two-dimensional region in the plane for a value of composition.[43,59,63] In this study, we perform MD simulations of an aqueous NaCl solution at various temperatures and pressures to determine the liquid-liquid coexistence region in the phase diagram. Such coexistence region has not been examined in the previous simulation studies. The coexistence region has also not been examined experimentally near the critical point because of rapid crystallization. We demonstrate that the NaCl solution separates into ion-rich and ion-poor parts spontaneously in MD simulations at several thermodynamic conditions. The degree of separation is quantified using the local density of the solute particles.

We also perform MD simulations of an aqueous Ne solution for comparison. Small hydrophobic molecules are almost immiscible with liquid water and aqueous solutions of them form clathrate hydrates quickly under high pressures. Therefore, it is difficult to examine the effect of hydrophobic particles on the phase behavior of supercooled water experimentally. We find that the aqueous Ne solution also separates into two immiscible liquids without formation of Ne

bubbles and clathrate hydrate, and the effect of Ne on the liquid-liquid coexistence pressure is opposite to that of NaCl.

COMPUTATIONAL DETAILS

The GROMACS 4.6 package is used for MD simulations.[64,65] The simulation time is 1000 ns at T = 252 and 260 K, and 2000 ns at lower temperatures. The particle mesh Ewald method is employed with a real space cutoff distance of 0.9 nm.[66,67] The temperature and the pressure are maintained using the Nose-Hoover method and the Berendsen method, respectively.[68–70] The dimension of the simulation cell along the z axis, L_z, is three times longer than the other two dimensions, L_x and L_y, so that the liquid-liquid interface formed in the cell becomes perpendicular to the z axis to minimize the surface area.

It has been reported that the liquid-liquid critical temperature of pure water is higher for nopolarizable five-site water models than for other types of water models.[2,25–30,51] This suggests that the dynamics of water around the critical temperature is fast for the five-site models. Indeed, we found that the time required for spontaneous liquid-liquid separation is much shorter for TIP5P than for TIP4P/2005 in the previous study.[38] It is expected that the simulation time required to observe liquid-liquid separation of aqueous solutions is also shorter for the five-site models. Therefore, we choose the TIP5P model in this study.[71] This model well reproduces the liquid structure.[72] The liquid-liquid critical point of pure TIP5P water is T_c, ~ 217 K and P_c, ~ 3400 bar.[26,38]

The aqueous NaCl solution consists of 60 Na^+, 60 Cl^-, and 1536 water molecules. The concentration of the solution is 2.2 mol kg^{-1}. All ions and water molecules are placed randomly in the initial configuration. A classical nonpolarizable model proposed by Dang is used for the ions (σ_{Na} = 0.2583 nm, ε_{Na} = 0.4184 kJ mol^{-1}, σ_{Cl} = 0.4401 nm, and ε_{Cl} = 0.4184 kJ mol^{-1}).[73] We also perform an MD simulation with a larger system containing 480 Na^+, 480 Cl^-, and 12288 water molecules to examine the system size effect.

The numbers of solute and water molecules in the aqueous Ne solution are 171 and 1536, respectively. The mole fraction of Ne is 0.1. The Lennard-Jones parameters of the solute are taken from a textbook (σ_{Ne} = 0.2749 nm and ε_{Ne} = 0.296 kJ mol^{-1}).[74]

RESULTS AND DISCUSSION

Figure 1 shows the initial and final configurations obtained from the MD simulation of the aqueous NaCl solution at T = 228 K and P = 1 bar. There exist an ion-poor region centered at z ~ 5 nm and an ion-rich region centered at z ~ 1.5 nm in the final state although the ions are randomly located in the initial state. We assume that a pair of Na^+ and Cl^- is bonded when the distance between them is shorter than 0.35 nm (this threshold corresponds to the first minimum of the Na^+-Cl^- radial distribution of crystalline NaCl). The ionic bonds are represented by thick green sticks in Fig. 1. There are only a few ionic bonds in the ion-rich region. This means that the separation is not due to crystallization of NaCl.

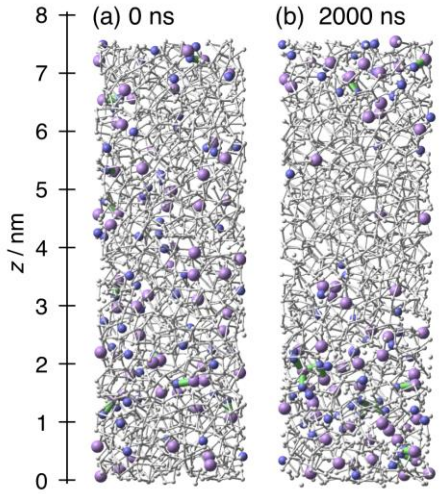

FIG. 1. (a) Initial and (b) final configurations of the MD simulation of the aqueous NaCl solution at T = 228 K and P = 1 bar. Blue and purple spheres represent Na^+ and Cl^-, respectively. Thick green sticks are ionic bonds between Na^+ and Cl^-. Water molecules and hydrogen bonds between them are represented by small light gray spheres and sticks. (Multimedia view)

We calculate the time-dependent number density profiles of Na^+ defined as

$$\rho(z,t) = \frac{1}{L_x L_x \Delta z} \sum_{i=1}^{n} \int_{z-\Delta z/2}^{z+\Delta z/2} \delta(z_i(t) - z')dz', \qquad (1)$$

with

$$\Delta z = \frac{L_z}{n_{bin}}, \qquad (2)$$

where $z_i(t)$ is the z coordinate of the i-th Na^+ particle, n is the number of Na^+ in the system, and n_{bin} is the number of bins. We set $n_{bin} = 20$. Figure 2a shows $\rho(z, t)$ at $T = 228$ K (the density profile of Cl^- is not shown because it is quite similar to the profile of Na^+). The spatial distribution of Na^+ is fairly uniform in the initial stage of the simulation. An ion-rich region centered at $z = 0.5$ nm forms at $t = 200$ ns. This region grows as time evolves. The ion-poor region left behind around $z = 4.5$ nm expands simultaneously. The separation process is also seen in the movie of Fig. 1 (Multimedia view).

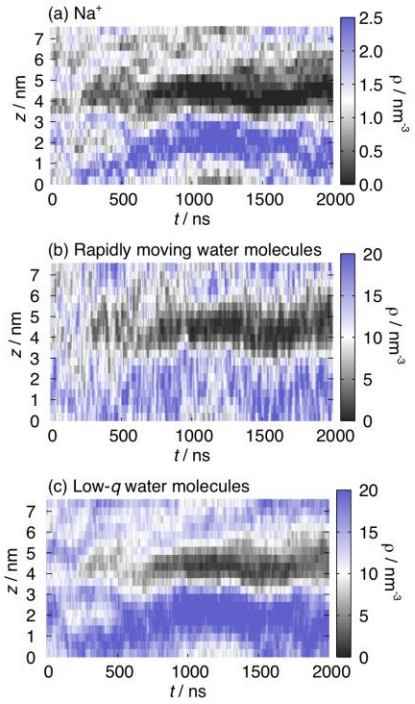

FIG. 2. Time dependent number density profiles of (a) Na^+, (b) rapidly moving water molecules, and (c) low-q water molecules in the aqueous NaCl solution at $T = 228$ K and $P = 1$ bar. The average number densities of Na^+ and whole water molecules are 1.25 and 32.0 nm^{-3}, respectively.

HDL and LDL can be distinguished by their dynamic properties; water molecules in HDL move faster than those in LDL.[15,16,38,75] We classify water molecules into rapidly and slowly moving molecules. A trajectory is divided into time bins with an interval of 1 ns, and the following quantity is calculated for each time bin

$$\delta_i^2(t) = \langle \{\mathbf{r}_i(t + \Delta t) - \mathbf{r}_i(t)\}^2 \rangle, \quad (3)$$

where $\mathbf{r}_i$ is the coordination vector of the oxygen atom of the i-th water molecule.[76–78] We set Δt = 0.1 ns. A water molecule is defined as a rapidly moving molecule when the $\delta_i^2(t)$ value is larger than that averaged over all molecules for each time bin. The time-dependent number density profile of the rapidly moving water molecules is presented in Fig. 2b. The ions are solvated in the region consisting of the rapidly moving molecules, i.e., HDL. This result is consistent with experimental results obtained for amorphous solids of aqueous LiCl solutions.[41–44]

HDL and LDL can also be distinguished by their structural properties; HDL is less structured than LDL.[2,38,79–82] We calculate the tetrahedrality parameter given by

$$q_i = 1 - \frac{3}{8}\sum_{j=1}^{3}\sum_{k=j+1}^{4}\left(\cos\theta_{jik} + \frac{1}{3}\right)^2, \quad (4)$$

where θ_{jik} is the angle between the two vectors connecting the central molecule, i, to two neighbors, j and k.[83] The value of q_i is maximized when the surrounding four molecules are located in a regular tetrahedral arrangement. We define that a water molecule is a low-q molecule when its q value is lower than that averaged over all molecules at each time step. Figure 2c shows the time-dependent number density profile of the low-q water molecules. As expected, the hydrogen bond network of the ion-rich region is less structured than that of the ion-poor region (The q parameter depends not only on the deviation of the O-O-O angle from 109.47° but also on the deviation of the number of hydrogen bonds from 4. As shown in Fig. S1, the low q parameter in the ion-rich region is because of the both contributions).

The time-dependent number density profiles of Na^+ at T = 236 K and 244 K are shown in Fig. 3. The difference in the number density of Na^+ between the ion-poor and ion-rich regions at T = 236 K is smaller than that at T = 228 K. The spatial distribution of Na^+ becomes almost uniform at T = 244 K. We quantify the degree of separation using the following expression:

$$d_s(t) = \frac{1}{n_{\mathrm{bin}}}\sum_{j=1}^{n_{\mathrm{bin}}}\left(\frac{\rho_j(t) - \langle\rho\rangle}{\langle\rho\rangle} + \frac{\rho_{j+1}(t) - \langle\rho\rangle}{\langle\rho\rangle}\right)^2 \quad (5)$$

where $\rho_j(t)$ is the local number density of Na^+ in the j-th spatial bin at t and $\langle\rho\rangle$ is the average number density. This quantity is large only when the local density of each spatial bin is significantly different from the averaged one and the local densities of neighboring bins are close to each other. The d_s value averaged over the last 500 ns of the simulation is 1.78, 0.93, and 0.52 for T = 228, 236, and 244 K, respectively.

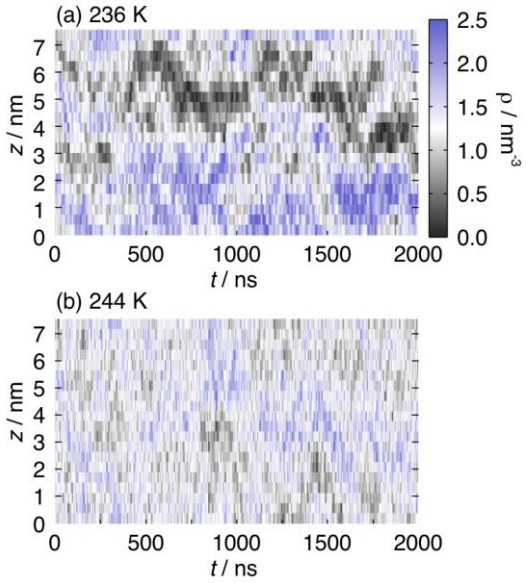

FIG. 3. Time-dependent number density profiles of Na^+ at (a) 236 K and (b) 244 K. The pressure is 1 bar.

MD simulations of the aqueous NaCl solution are performed at pressures ranging from –1200 bar to 3200 bar at T = 228, 232, 236, 240, 244, 248, 252, and 260 K. Figure 4a shows the d_s values of these simulations. The d_s value is large at low temperatures and low pressures. The non-monotonic pressure-dependence found at 228 K and 232 K can be attributed to the slow dynamics of water at these low temperatures shown in Fig. S2 and the fairly large fluctuations of ds shown in Fig. S3 (the pressure-dependence would be smooth and monotonic if the simulations are elongated but it is not the aim of this study). As shown in Fig. 3a, there are two liquid phases in the system at T = 236 K and P = 1 bar but the interface between the two phases is not so clear. This suggests that the system would become single-phase if the temperature is somewhat increased. We assume tentatively that there are two immiscible liquids in the system when the d_s value is larger than 0.9 which is slightly smaller than the value at T = 236 K and P = 1 bar of 0.93. Figure 4b is a schematic representation of the phase diagram of the NaCl solution based on the d_s values (A small change in the threshold d_s value only causes a small change in the area of the two-phase coexistence region in the phase diagram. More precise phase diagrams would be obtained if sophisticated schemes such as the grand canonical Monte Carlo method are employed, but it is beyond the scope of this study). The effect of NaCl on the phase diagram of supercooled water is remarkable. The liquid-liquid coexistence of the NaCl solution occurs up to at least 240 K, which

is much higher than the critical point of pure TIP5P water. This indicates that the stabilization caused by the ions is larger for either or both of the two coexistence phases than for the liquid-liquid supercritical fluid because a decrease in the chemical potential of a phase results in expansion of its stable region in the phase diagram. The liquid-liquid coexistence pressure is lower for the NaCl solution than for pure water. This means that the solute stabilizes the HDL phase more than the LDL phase. Hydration of ions involves reorientation of water molecules, which results in lowering of the ion-water interaction energy. This effect is more pronounced for less structured liquids in which solvent molecules are loosely bound by other solvent molecules. Therefore, the stabilization caused by the ions is larger for HDL than for LDL and for the liquid-liquid supercritical fluid that is partly LDL-like.

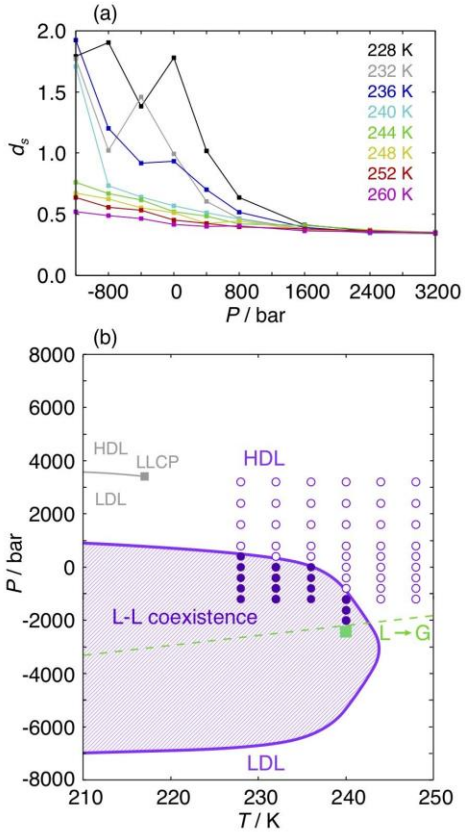

FIG. 4. (a) Degree of separation, d_s, for the aqueous NaCl solution. The d_s value is averaged over the last 500 ns of the simulation. (b) Schematic representation of the phase diagram for the aqueous NaCl solution. The circles show the pressures and temperatures examined. The circles are filled when the d_s value is larger than 0.9. Cavitation occurs very quickly at the point marked by the green square. The green dashed line indicates schematically the limit of stability of the liquid. The phase diagram of pure TIP5P water is shown in gray.

The whole aqueous NaCl solution should become LDL when the pressure is low enough. To examine this, we perform MD simulations at pressures lower than –1200 bar at T = 240 K. The liquid-liquid coexistence is observed at P = –1600, –2000, and –2400 bar. At P = –2800 bar, however, cavitation occurs very quickly in the solution. Probably, it is impossible to realize the pure LDL state of the NaCl solution at any pressure because of the quick cavitation in the deeply negative pressure region for the force field models employed in this study.

The aqueous Ne solution also separates into two parts. Figure 5 presents the initial and final configurations of the MD simulation at T = 228 K and P = 8000 bar. There are a Ne-rich region and a Ne-poor region in the final state. The density of water is ~0.95 g/ml and the mole fraction of Ne is roughly 0.2 in the Ne-rich region, indicating that this region is not a Ne fluid but an aqueous solution. We search for the 5^{12}, $5^{12}6^2$, and $5^{12}6^4$ hydrate cages using the algorithm proposed Jacobson *et al.*,[84,85] and confirm that there is no hydrate cage in the final configuration. These results indicate that the observed separation process is neither due to bubble (or droplet) formation of Ne nor formation of clathrate hydrate. The time-dependent density profiles of the solute particles, rapidly moving water molecules, and low-q water molecules in the aqueous Ne solution are shown in Fig. 6. The dynamics of water in the Ne-rich region is slower than that in the Ne-poor region and the Ne-rich region is more structured than the Ne-poor region: Ne is mostly solvated in LDL.

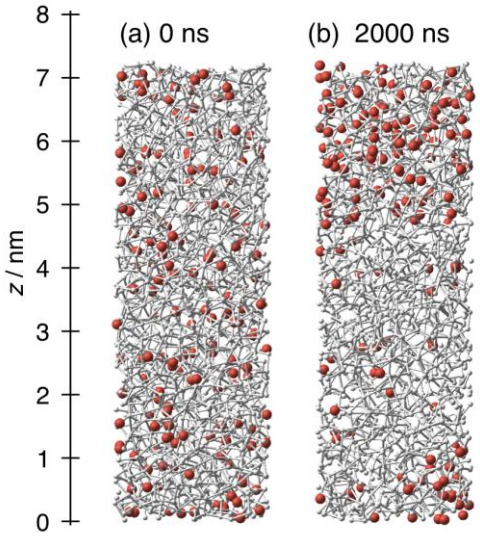

FIG. 5. (a) Initial and (b) final configurations of the MD simulation of the aqueous Ne solution at T = 228 K and P = 8000 bar. Ne molecules are represented by red spheres.

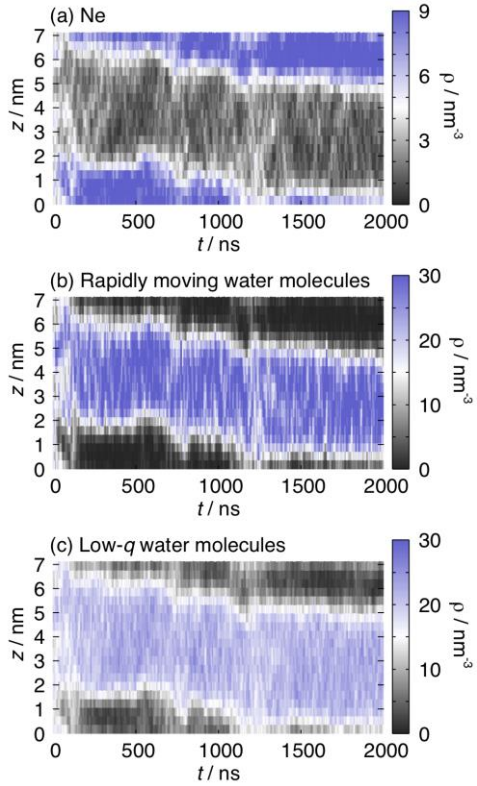

FIG. 6. Time-dependent number density profiles of (a) Ne, (b) rapidly moving water molecules, and (c) low-q water molecules in the aqueous Ne solution at T = 228 K and P = 8000 bar. The average number densities of Ne and whole water molecules are 4.29 and 38.5 nm^{-3}, respectively.

Figure 7a shows the d_s values of the simulations of the aqueous Ne solution. The d_s value is large at low temperatures and high pressures. Figure 7b shows the schematic phase diagram of the aqueous Ne solution. The liquid-liquid coexistence pressure of the Ne solution is higher than that of pure water, and the high-temperature limit of the liquid-liquid coexistence for the Ne solution is higher than that for pure water. This behavior suggests that Ne stabilizes the LDL phase more than the HDL phase and the liquid-liquid supercritical fluid. Solubility of small hydrophobic molecules is mainly determined by the insertion probability, which is defined as the ratio of the volume of cavities that can include the solute in a unit volume.[86–88] Thus, Ne is preferentially solvated in LDL,[62] and water molecules in LDL is stabilized by the interactions with Ne molecules in a way similar to those in clathrate hydrate.[89,90]

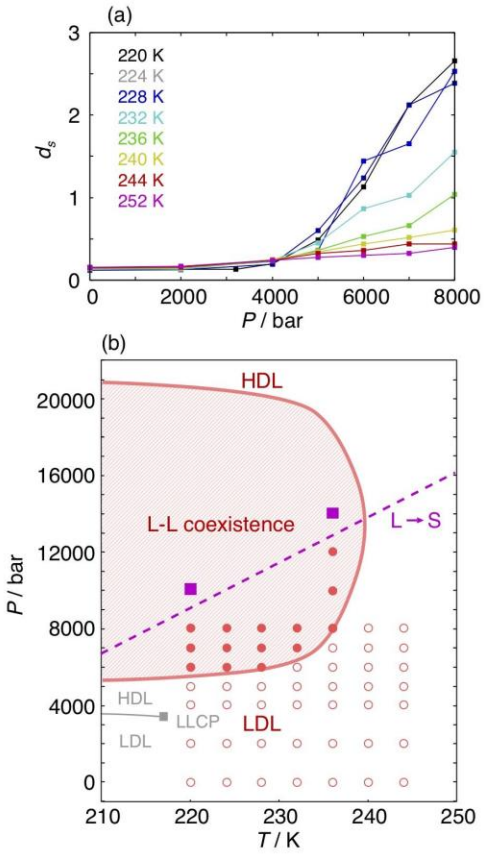

FIG. 7. (a) Degree of separation, d_s, for the aqueous Ne solution. (b) Schematic representation of the phase diagram for the aqueous Ne solution. The circles show the pressures and temperatures examined. The circles are filled when the liquid separates into two parts ($d_s > 0.9$). Ice T2 forms very quickly at the points marked by the purple squares. The purple dashed line indicates the limit of stability of the liquid. The phase diagram of pure TIP5P water is shown in gray.

The most stable solid phase at pressures higher than 10000 bar is either ice VI or ice VII (ignoring hydrogen-ordered phases). In computer simulations using classical water models, however, crystalline structures that have not been prepared experimentally can be more stable than ice VI and VII,[77,91–94] probably because of the Lennard-Jones potential used instead of more precise functions such as the exp-6 Buckingham function.[95] Ice T2 is one of such unreal high-pressure ice crystals.[77] This ice occupies a wide area as the most stable state in the high-pressure region of the phase diagram of TIP5P water. The structure is quite complex: its unit cell consisting of 152 water molecules is larger than that of any ice phases that can be prepared experimentally. Ice T2 forms without any induction time when the pressure is quite high and the temperature is low enough. We

observe that the Ne-poor region freezes into a solid quickly at points marked by the purple squares in Fig. 7b. The O-O radial distribution function implies that this solid is ice T2 or similar unreal ice phases (Fig. S4), although we cannot identify it precisely due to very small grain sizes caused by the high driving force for the phase transition. Because of this phase transition, it is impossible (or quite difficult) to reach the pure HDL state of the aqueous Ne solution that would exist in the very high pressure region.

We finally discuss the effect of the system size. Figure 8b shows the final configuration of the MD simulation of the NaCl solution with a larger system size starting from a random configuration. The cell dimensions of the larger system are twice those of the smaller system. The temperature, pressure, and concentration of NaCl are the same as those of the MD simulation shown in Fig. 1. It is found that there are ion-rich and ion-poor regions in the final configuration. However, the final configuration is far away from the completely separated state in which two liquid slabs are divided by two flat surfaces that are perpendicular to the *z*-axis (there must be two surfaces because of the periodic boundary conditions). A longer simulation time is required to achieve the completely separated state because the ions need to move longer distance in the larger system.

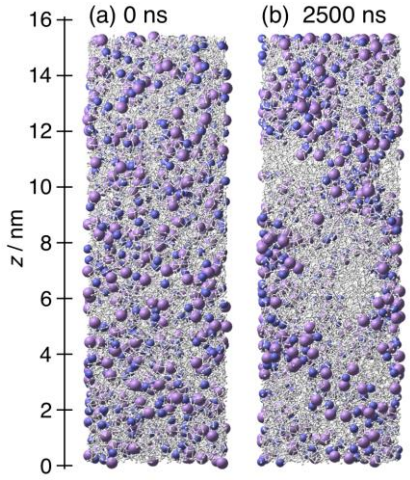

FIG. 8. (a) Initial and (b) final configurations of the MD simulation of the aqueous NaCl solution with a larger system size. The temperature and pressure are T = 228 K and P = 1 bar.

CONCLUSIONS

We have investigated supercooled aqueous NaCl and Ne solutions using MD simulations. It is demonstrated that the NaCl solution separates into ion-rich and ion-poor parts when the

temperature and pressure are low enough. Analyses of the structure and dynamics of water show that the ion-rich and ion-poor parts correspond to HDL and LDL, respectively. The aqueous Ne solution also separates into two solutions. In contrast to the ions, Ne is mostly solvated in LDL and the liquid-liquid separation occurs at high pressures.

The highest temperature at which the liquid-liquid coexistence occurs is higher than the critical point of pure water for the two aqueous solutions. The temperature may be even higher for an aqueous solution including both NaCl and Ne. If so, it may be possible to observe the liquid-liquid separation experimentally without crystallization. It is also interesting to investigate supercooled solutions of different ions. The effect of small divalent ions, such as Mg^{2+}, may be larger than that of the monovalent ions. MD simulations of the liquid-liquid coexistence of these systems may shed a new light on the phase behavior of aqueous supercooled solutions.

In this study, we employ only one set of force field models: TIP5P for water, Dang's parameters for NaCl, and the LJ parameters taken from the textbook of Hirschfelder, Curtiss, and Bird for Ne. Thermodynamics properties depend strongly on potential parameters. The effects of NaCl and Ne on supercooled water found in this study, such as the increase in the liquid-liquid separation temperature, will be observed for different force field models. However, the effects can be quantitatively quite different. For example, the increase in the liquid-liquid separation temperature might be pronounced by the increase in the hydration free energy of ion that can be caused by the increase in the partial charge of water molecules or the decrease in the LJ size parameter of ion. It is unclear which is significant for the effects of solute on liquid-liquid separation among parameters of force field models. This issue should be investigated in future work.

MD simulation studies have reported that crystallization occurs preferentially in the LDL (or LDL-like) region for pure liquid water and Si.[38,96] The liquid-liquid separation of aqueous solutions may also affect some crystallization processes. The local concentration of the guest molecules should be high enough in the solution to form nuclei or amorphous precursors of clathrate hydrate.[85,97–100] Similarly, the local concentration of the ions should be high in the solution for nucleation or precursor formation of rock salt.[101,102] Large fluctuations of the local concentration of the solute arising from the liquid-liquid phase transition may be relevant to these processes.

SUPPLEMENTARY MATERIAL

See Supplementary Material for the coordination number and the O-O-O angle of water molecules in HDL and LDL, the hydrogen bond autocorrelation functions of water, the standard deviation of the degree of separation, and the radial distribution function of the solid formed in the solute-poor region of the aqueous Ne solution at T = 240 K and P = 14000 bar.

ACKNOWLEDGMENTS

The present work was supported by JSPS KAKENHI Grant No. 16K05658 and MEXT as “Priority Issue on Post-Kcomputer” (Development of new fundamental technologies for high-efficiency energy creation, conversion/storage and use) using computational resources of the K computer provided by the RIKEN Advanced Institute for Computational Science through the HPCI System Research project (Project ID: hp180204). MD simulations were also performed on the computers at Research Center for Computational Science, Okazaki, Japan.

REFERENCES

[1] O. Mishima, L.D. Calvert, and E. Whalley, Nature **314**, 76 (1985).

[2] P.H. Poole, F. Sciortino, U. Essmann, and H. Eugene Stanley, Nature **360**, 324 (1992).

[3] C.A. Angell, W.J. Sichina, and M. Oguni, J. Phys. Chem. **86**, 998 (1982).

[4] O. Mishima and H. Eugene Stanley, Nature **396**, 329 (1998).

[5] J.C. Palmer, P.H. Poole, F. Sciortino, and P.G. Debenedetti, Chem. Rev. **118**, 9129 (2018).

[6] S. Saito, B. Bagchi, and I. Ohmine, J. Chem. Phys. **149**, 124504 (2018).

[7] I. Okabe I., H. Tanaka, and K. Nakanishi, Phys. Rev. E Stat. Phys. Plasmas Fluids Relat. Interdiscip. Topics **53**, 2638 (1996).

[8] J. Bai and X.C. Zeng, Proc. Natl. Acad. Sci. U. S. A. **109**, 21240 (2012).

[9] O. Mishima, J. Chem. Phys. **100**, 5910 (1994).

[10] O. Mishima, Phys. Rev. Lett. **85**, 334 (2000).

[11] O. Mishima and H. Eugene Stanley, Nature **392**, 164 (1998).

[12] K. Ito, C.T. Moynihan, and C. Austen Angell, Nature **398**, 492 (1999).

[13] F. Mallamace, C. Corsaro, M. Broccio, C. Branca, N. González-Segredo, J. Spooren, S.-H. Chen, and H.E. Stanley, Proc. Natl. Acad. Sci. U. S. A. **105**, 12725 (2008).

[14] F. Mallamace, M. Broccio, C. Corsaro, A. Faraone, D. Majolino, V. Venuti, L. Liu, C.-Y. Mou, and S.-H. Chen, Proc. Natl. Acad. Sci. U. S. A. **104**, 424 (2007).

[15] A. Faraone, L. Liu, C.-Y. Mou, C.-W. Yen, and S.-H. Chen, J. Chem. Phys. **121**, 10843 (2004).

[16] L. Liu, S.-H. Chen, A. Faraone, C.-W. Yen, and C.-Y. Mou, Phys. Rev. Lett. **95**, 117802 (2005).

[17] M. Matsumoto, S. Saito, and I. Ohmine, Nature **416**, 409 (2002).

[18] E. Sanz, C. Vega, J.R. Espinosa, R. Caballero-Bernal, J.L.F. Abascal, and C. Valeriani, J. Am. Chem. Soc. **135**, 15008 (2013).

[19] J.R. Espinosa, E. Sanz, C. Valeriani, and C. Vega, J. Chem. Phys. **141**, 18C529 (2014).

[20] J.C. Palmer, P.H. Poole, F. Sciortino, and P.G. Debenedetti, Chem. Rev. **118**, 9129 (2018).

[21] E.B. Moore and V. Molinero, Nature **479**, 506 (2011).

[22] L. Lupi, A. Hudait, B. Peters, M. Grünwald, R. Gotchy Mullen, A.H. Nguyen, and V. Molinero, Nature **551**, 218 (2017).

[23] A. Haji-Akbari and P.G. Debenedetti, Proceedings of the National Academy of Sciences **112**, 10582 (2015).

[24] A. Haji-Akbari and P.G. Debenedetti, Proceedings of the National Academy of Sciences **114**, 3316 (2017).

[25] S. Harrington, R. Zhang, P.H. Poole, F. Sciortino, and H. Eugene Stanley, Phys. Rev. Lett. **78**, 2409 (1997).

[26] M. Yamada, S. Mossa, H.E. Stanley, and F. Sciortino, Phys. Rev. Lett. **88**, 195701 (2002).

[27] I. Brovchenko, A. Geiger, and A. Oleinikova, J. Chem. Phys. **123**, 044515 (2005).

[28] D. Paschek, A. Rüppert, and A. Geiger, Chemphyschem **9**, 2737 (2008).

[29] J.L.F. Abascal and C. Vega, J. Chem. Phys. **133**, 234502 (2010).

[30] T. Sumi and H. Sekino, RSC Adv. **3**, 12743 (2013).

[31] Y. Liu, A.Z. Panagiotopoulos, and P.G. Debenedetti, J. Chem. Phys. **131**, 104508 (2009).

[32] F. Sciortino, I. Saika-Voivod, and P.H. Poole, Phys. Chem. Chem. Phys. **13**, 19759 (2011).

[33] P.H. Poole, R.K. Bowles, I. Saika-Voivod, and F. Sciortino, J. Chem. Phys. **138**, 034505 (2013).

[34] J.C. Palmer, F. Martelli, Y. Liu, R. Car, A.Z. Panagiotopoulos, and P.G. Debenedetti, Nature **510**, 385 (2014).

[35] J.C. Palmer, A. Haji-Akbari, R.S. Singh, F. Martelli, R. Car, A.Z. Panagiotopoulos, and P.G. Debenedetti, J. Chem. Phys. **148**, 137101 (2018).

[36] T.A. Kesselring, E. Lascaris, G. Franzese, S.V. Buldyrev, H.J. Herrmann, and H.E. Stanley, J. Chem. Phys. **138**, 244506 (2013).

[37] T.A. Kesselring, G. Franzese, S.V. Buldyrev, H.J. Herrmann, and H.E. Stanley, Sci. Rep. **2**, 474 (2012).

[38] T. Yagasaki, M. Matsumoto, and H. Tanaka, Phys. Rev. E Stat. Nonlin. Soft Matter Phys. **89**, 020301 (2014).

[39] J. Guo, R.S. Singh, and J.C. Palmer, Mol. Phys. **116**, 1953 (2018).

[40] C.A. Angell and E.J. Sare, J. Chem. Phys. **49**, 4713 (1968).

[41] Y. Suzuki and O. Mishima, Phys. Rev. Lett. **85**, 1322 (2000).

[42] O. Mishima, J. Chem. Phys. **126**, 244507 (2007).

[43] Y. Suzuki and O. Mishima, J. Chem. Phys. **138**, 084507 (2013).

[44] O. Mishima, J. Phys. Chem. B **115**, 14064 (2011).

[45] S. Woutersen, B. Ensing, M. Hilbers, Z. Zhao, and C.A. Angell, Science **359**, 1127 (2018).

[46] Y. Suzuki and O. Mishima, J. Chem. Phys. **141**, 094505 (2014).

[47] Y. Suzuki, J. Chem. Phys. **147**, 064511 (2017).

[48] Y. Suzuki, J. Chem. Phys. **149**, 204501 (2018).

[49] J. Bachler, V. Fuentes-Landete, D.A. Jahn, J. Wong, N. Giovambattista, and T. Loerting, Phys. Chem. Chem. Phys. **18**, 11058 (2016).

[50] K.-I. Murata and H. Tanaka, Nat. Mater. **11**, 436 (2012).

[51] N.J. Hestand and J.L. Skinner, J. Chem. Phys. **149**, 140901 (2018).

[52] O. Mishima, J. Chem. Phys. **133**, 144503 (2010).

[53] V. Holten, C.E. Bertrand, M.A. Anisimov, and J.V. Sengers, J. Chem. Phys. **136**, 094507 (2012).

[54] D. Corradini, M. Rovere, and P. Gallo, J. Chem. Phys. **132**, 134508 (2010).

[55] D. Corradini and P. Gallo, J. Phys. Chem. B **115**, 14161 (2011).

[56] D. Corradini, Z. Su, H.E. Stanley, and P. Gallo, J. Chem. Phys. **137**, 184503 (2012).

[57] D. Corradini, S.V. Buldyrev, P. Gallo, and H.E. Stanley, Phys. Rev. E Stat. Nonlin. Soft Matter Phys. **81**, 061504 (2010).

[58] L. Le and V. Molinero, J. Phys. Chem. A **115**, 5900 (2011).

[59] J.W. Biddle, V. Holten, and M.A. Anisimov, J. Chem. Phys. **141**, 074504 (2014).

[60] D.A. Jahn, J. Wong, J. Bachler, T. Loerting, and N. Giovambattista, Phys. Chem. Chem. Phys. **18**, 11042 (2016).

[61] S. Chatterjee and P.G. Debenedetti, J. Chem. Phys. **124**, 154503 (2006).

[62] D. Paschek, Phys. Rev. Lett. **94**, 217802 (2005).

[63] T. Driesner and C.A. Heinrich, Geochim. Cosmochim. Acta **71**, 4880 (2007).

[64] B. Hess, C. Kutzner, D. van der Spoel, and E. Lindahl, J. Chem. Theory Comput. **4**, 435 (2008).

[65] D. Van Der Spoel, E. Lindahl, B. Hess, G. Groenhof, A.E. Mark, and H.J.C. Berendsen, J. Comput. Chem. **26**, 1701 (2005).

[66] T. Darden, D. York, and L. Pedersen, J. Chem. Phys. **98**, 10089 (1993).

[67] U. Essmann, L. Perera, M.L. Berkowitz, T. Darden, H. Lee, and L.G. Pedersen, J. Chem. Phys. **103**, 8577 (1995).

[68] S. Nosé, Mol. Phys. **52**, 255 (1984).

[69] W.G. Hoover, Phys. Rev. A **31**, 1695 (1985).

[70] H.J.C. Berendsen, J.P.M. Postma, W.F. van Gunsteren, A. DiNola, and J.R. Haak, J. Chem. Phys. **81**, 3684 (1984).

[71] M.W. Mahoney and W.L. Jorgensen, J. Chem. Phys. **112**, 8910 (2000).

[72] C. Vega, C. McBride, E. Sanz, and J.L.F. Abascal, Phys. Chem. Chem. Phys. **7**, 1450 (2005).

[73] L.X. Dang, J. Am. Chem. Soc. **117**, 6954 (1995).

[74] J.O. Hirschfelder, C.F. Curtiss, and R.B. Bird, *Molecular Theory of Gases and Liquids* (Wiley, New York, 1954).

[75] L. Xu, P. Kumar, S.V. Buldyrev, S.-H. Chen, P.H. Poole, F. Sciortino, and H.E. Stanley, Proc. Natl. Acad. Sci. U. S. A. **102**, 16558 (2005).

[76] J. Vatamanu and P.G. Kusalik, J. Chem. Phys. **126**, 124703 (2007).

[77] T. Yagasaki, M. Matsumoto, and H. Tanaka, J. Phys. Chem. B **122**, 7718 (2018).

[78] T. Yagasaki, M. Matsumoto, and H. Tanaka, J. Phys. Chem. B **122**, 3396 (2018).

[79] N. Giovambattista, H.E. Stanley, and F. Sciortino, Phys. Rev. E Stat. Nonlin. Soft Matter Phys. **72**, 031510 (2005).

[80] D.T. Bowron, J.L. Finney, A. Hallbrucker, I. Kohl, T. Loerting, E. Mayer, and A.K. Soper, J. Chem.

Phys. **125**, 194502 (2006).

[81] K. Amann-Winkel, M.-C. Bellissent-Funel, L.E. Bove, T. Loerting, A. Nilsson, A. Paciaroni, D. Schlesinger, and L. Skinner, Chem. Rev. **116**, 7570 (2016).

[82] H. Tanaka, Phys. Rev. Lett. **80**, 113 (1998).

[83] J.R. Errington and P.G. Debenedetti, Nature **409**, 318 (2001).

[84] L.C. Jacobson, W. Hujo, and V. Molinero, J. Phys. Chem. B **113**, 10298 (2009).

[85] T. Yagasaki, M. Matsumoto, and H. Tanaka, J. Phys. Chem. C **120**, 21512 (2016).

[86] B. Widom, J. Phys. Chem. **86**, 869 (1982).

[87] A. Pohorille and L.R. Pratt, J. Am. Chem. Soc. **112**, 5066 (1990).

[88] D. Chandler, Nature **437**, 640 (2005).

[89] H. Tanaka, T. Yagasaki, and M. Matsumoto, J. Chem. Phys. **149**, 074502 (2018).

[90] E.D. Sloan and C.A. Koh, *Clathrate Hydrates of Natural Gases* (CRC Press, Boca Raton, 2008).

[91] Y. Takii, K. Koga, and H. Tanaka, J. Chem. Phys. **128**, 204501 (2008).

[92] J.L. Aragones and C. Vega, J. Chem. Phys. **130**, 244504 (2009).

[93] K. Mochizuki, K. Himoto, and M. Matsumoto, Phys. Chem. Chem. Phys. **16**, 16419 (2014).

[94] M. Hirata, T. Yagasaki, M. Matsumoto, and H. Tanaka, Langmuir **33**, 11561 (2017).

[95] C. Vega and J.L.F. Abascal, Phys. Chem. Chem. Phys. **13**, 19663 (2011).

[96] C. Desgranges and J. Delhommelle, J. Am. Chem. Soc. **133**, 2872 (2011).

[97] L.C. Jacobson, W. Hujo, and V. Molinero, J. Am. Chem. Soc. **132**, 11806 (2010).

[98] B.C. Knott, V. Molinero, M.F. Doherty, and B. Peters, J. Am. Chem. Soc. **134**, 19544 (2012).

[99] S. Liang and P.G. Kusalik, J. Phys. Chem. B **117**, 1403 (2013).

[100] Z. Zhang, M.R. Walsh, and G.-J. Guo, Phys. Chem. Chem. Phys. **17**, 8870 (2015).

[101] D. Chakraborty and G.N. Patey, J. Phys. Chem. Lett. **4**, 573 (2013).

[102] H. Jiang, A. Haji-Akbari, P.G. Debenedetti, and A.Z. Panagiotopoulos, J. Chem. Phys. **148**, 044505 (2018).